Evidence of Coherent K^{+} Meson Production in Neutrino-Nucleus Scattering

Z. Wang *et al.* (MINERvA Collaboration)

Phys. Rev. Lett. **117**, 061802 — Published 5 August 2016

DOI: 10.1103/PhysRevLett.117.061802

First evidence of coherent K^+ meson production in neutrino-nucleus scattering

Z. Wang,[1] C.M. Marshall,[1] L. Aliaga,[2,3] O. Altinok,[4] L. Bellantoni,[5] A. Bercellie,[1] M. Betancourt,[5] A. Bodek,[1] A. Bravar,[6] H. Budd,[1] T. Cai,[1] M.F. Carneiro,[7] H. da Motta,[7] S.A. Dytman,[8] G.A. Díaz,[1,3] B. Eberly,[8,*] E. Endress,[3] J. Felix,[9] L. Fields,[5,10] R. Fine,[1] R.Galindo,[11] H. Gallagher,[4] A. Ghosh,[11,7] T. Golan,[1,5] R. Gran,[12] D.A. Harris,[5] A. Higuera,[1,9,†] K. Hurtado,[7,13] M. Kiveni,[5] J. Kleykamp,[1] M. Kordosky,[2] T. Le,[4,14] E. Maher,[15] S. Manly,[1] W.A. Mann,[4] D.A. Martinez Caicedo,[7,‡] K.S. McFarland,[1,5] C.L. McGivern,[8,§] A.M. McGowan,[1] B. Messerly,[8] J. Miller,[11] A. Mislivec,[1] J.G. Morfín,[5] J. Mousseau,[16,¶] D. Naples,[8] J.K. Nelson,[2] A. Norrick,[2] Nuruzzaman,[14,11] V. Paolone,[8] J. Park,[1] C.E. Patrick,[10] G.N. Perdue,[5,1] L. Rakotondravohitra,[5,**] M.A. Ramirez,[9] R.D. Ransome,[14] H. Ray,[16] L. Ren,[8] D. Rimal,[16] P.A. Rodrigues,[1] D. Ruterbories,[1] H. Schellman,[17,10] D.W. Schmitz,[18,5] C. Simon,[19] C.J. Solano Salinas,[13] B.G. Tice,[14] E. Valencia,[9] T. Walton,[20,††] J. Wolcott,[1,‡‡] M.Wospakrik,[16] G. Zavala,[9,§§] and D. Zhang[2]

(MINERvA Collaboration)

[1] *University of Rochester, Rochester, New York 14627 USA*
[2] *Department of Physics, College of William & Mary, Williamsburg, Virginia 23187, USA*
[3] *Sección Física, Departamento de Ciencias, Pontificia Universidad Católica del Perú, Apartado 1761, Lima, Perú*
[4] *Physics Department, Tufts University, Medford, Massachusetts 02155, USA*
[5] *Fermi National Accelerator Laboratory, Batavia, Illinois 60510, USA*
[6] *University of Geneva, 1211 Geneva 4, Switzerland*
[7] *Centro Brasileiro de Pesquisas Físicas, Rua Dr. Xavier Sigaud 150, Urca, Rio de Janeiro, Rio de Janeiro, 22290-180, Brazil*
[8] *Department of Physics and Astronomy, University of Pittsburgh, Pittsburgh, Pennsylvania 15260, USA*
[9] *Campus León y Campus Guanajuato, Universidad de Guanajuato, Lascurain de Retana No. 5, Colonia Centro, Guanajuato 36000, Guanajuato México.*
[10] *Northwestern University, Evanston, Illinois 60208*
[11] *Departamento de Física, Universidad Técnica Federico Santa María, Avenida España 1680 Casilla 110-V, Valparaíso, Chile*
[12] *Department of Physics, University of Minnesota – Duluth, Duluth, Minnesota 55812, USA*
[13] *Universidad Nacional de Ingeniería, Apartado 31139, Lima, Perú*
[14] *Rutgers, The State University of New Jersey, Piscataway, New Jersey 08854, USA*
[15] *Massachusetts College of Liberal Arts, 375 Church Street, North Adams, MA 01247*
[16] *University of Florida, Department of Physics, Gainesville, FL 32611*
[17] *Department of Physics, Oregon State University, Corvallis, Oregon 97331, USA*
[18] *Enrico Fermi Institute, University of Chicago, Chicago, IL 60637 USA*
[19] *Department of Physics and Astronomy, University of California, Irvine, Irvine, California 92697-4575, USA*
[20] *Hampton University, Dept. of Physics, Hampton, VA 23668, USA*

(Dated: July 12, 2016)

Neutrino-induced charged-current coherent kaon production, $\nu_\mu A \to \mu^- K^+ A$, is a rare, inelastic electroweak process that brings a K^+ on shell and leaves the target nucleus intact in its ground state. This process is significantly lower in rate than neutrino-induced charged-current coherent pion production, because of Cabibbo suppression and a kinematic suppression due to the larger kaon mass. We search for such events in the scintillator tracker of MINERvA by observing the final state K^+, μ^- and no other detector activity, and by using the kinematics of the final state particles to reconstruct the small momentum transfer to the nucleus, which is a model-independent characteristic of coherent scattering. We find the first experimental evidence for the process at 3σ significance.

PACS numbers: 13.15.+g,25.30.Pt

Charged mesons may be produced in inelastic, coherent charged-current reactions of neutrinos. This reaction is believed to occur when an off-shell W boson fluctuates to a meson. The meson is brought on the mass shell by exchange of a particle carrying no quantum numbers with the target nucleus, as illustrated in Fig. 1. Charged pion production through this mechanism has been observed and measured with $\mathcal{O}(10)\%$ precision on nuclei ranging from carbon to argon and across a range of neutrino (and antineutrino) energies from a few GeV to tens of GeV [1–8]. If the mechanism described above is the source of these events, then there should be an analogous, Cabibbo-suppressed process in which a $K^\pm$ meson is produced. In this Letter, we report the first experimental evidence of this process.

The exchange with the nucleus must leave the nucleus in its ground state for the process to be coherent. This requires that the four momentum transfer to the nucleus,

$\Delta p_N \equiv p_{Af} - p_{Ai}$, satisfy the relation $|t| \equiv \left|(\Delta p_N)^2\right| \leq \hbar^2/R^2$, where R is the radius of the nucleus. Adler's theorem [9] relates the coherent meson production cross section at $Q^2 \equiv -q^2 = 0$ to the meson-nucleus elastic cross section [10–12]. In the limit of muon and meson masses $m_\mu, m_M \ll E_\nu$, where E_ν is the neutrino energy,

$$\left.\frac{d^3\sigma_{coh}}{dQ^2 dy\, d|t|}\right|_{Q^2=0} = \frac{G_F^2}{2\pi^2} f_M^2 \frac{1-y}{y} \frac{d\sigma(MA \to MA)}{d|t|}, \quad (1)$$

where E_M is the final state meson energy, $y = E_M/E_\nu$, and f_M is the meson decay constant. The meson-nucleus elastic cross section and its exponential decrease with increasing $|t|$ are parameterized from meson-nucleus scattering data [11–17]. Models must be used to extrapolate away from $Q^2 = 0$. The model most commonly used in neutrino event generators [14–17] is that of Rein and Sehgal [12], which assumes no vector current and extrapolates the axial-vector current using a multiplicative dipole form factor $F^2_{dipole}(Q^2) = 1/(1 + Q^2/m_A^2)^2$ to modify Eq. 1. Other authors have proposed alternate extrapolations away from $Q^2 = 0$ [13, 18–20]. At low energies, modifications to Eq. 1 due to finite masses become important, restricting the allowed kinematics to $Q^2 \geq m_\mu^2 \frac{y}{1-y}$ and $|t| \geq \left(\frac{Q^2+m_M^2}{2yE_\nu}\right)^2$ [21, 22]. This restriction on $|t|$ removes more phase space for kaon production than it does for pion production due to the larger meson mass, m_M. An alternate approach is to start with the Cabibbo-suppressed single kaon production cross section on nucleons [23] at low neutrino energies and calculate a coherent sum [24].

Standard neutrino interaction generators [14–17] have no model for coherent K^+ production. Even in PCAC models, the dearth of data on low energy K^+-nucleus elastic scattering at the relevant kaon energies [25, 26] precludes a precise calculation. However, the rate in the signal model does not affect the result, and in fact the model is only needed to determine energy deposited near the interaction point and the distribution of $|t|$, and both of those quantities are most affected by well-modeled detector resolutions. Therefore, we generate coherent pion production with GENIE 2.8.4 [14] and recalculate hadronic kinematics while holding the lepton kinematics and magnitude of the four-momentum transfer to the nucleus fixed. The larger kaon mass means there is only a physical solution for 26% of pion events for MINERvA's neutrino flux. The rate is also reduced by a factor of $(f_K/f_\pi)^2 \tan^2\theta_C = 0.077 \pm 0.001$ [27], where θ_C is the Cabibbo angle. The ratio of the K^+ to π^+ elastic scattering cross sections on carbon is calculated to be ~ 0.7 [28], consistent with measurements at higher meson energies [25]. We therefore expect our flux- averaged cross section for coherent K^+ production to be $\sim 4 \times 10^{41}$ cm^2 per carbon nucleus.

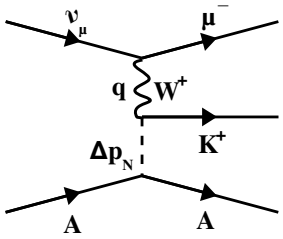

FIG. 1: Feynman diagram for coherent charged kaon production. The square of the momentum transfer to the nucleus is $|\Delta p_N|^2 = |q - p_K|^2 = |t|$.

The signal reaction produces events with a forward K^+ and μ^- and no additional energy near the vertex. Processes that produce the same final state, but often with additional low energy particles at the interaction vertex and with large $|t|$, are simulated using the GENIE 2.8.4 neutrino event generator [14]. Inelastic reactions for $W < 1.7$ GeV are simulated with a tuned model of discrete baryon resonance production [29]. The transition to deep inelastic scattering is simulated using the Bodek-Yang model [30]. Hadronization at higher energies is simulated with the AGKY model [31] based on the gradual transition from KNO scaling [32] to the LUND string model of PYTHIA [33] with increasing final state hadronic invariant mass, W. In GENIE, parameters that control the rate of strange particle production in hadronization are tuned such that rates of Λ and K^0_S production on deuterium and neon agree with bubble chamber measurements [34–39]. Final state interactions, in which hadrons interact within the target nucleus, are modeled using the INTRANUKE package [14]. GENIE does not simulate FSI processes where K^+ are produced in π^+ interactions, for example $\pi^+ n \to K^+\Lambda$. However, π^+ strong interactions can only produce pairs of strage particles, and Λ or Σ baryons will cause events to be rejected.

Cabibbo-suppressed $\Delta S = 1$ reactions are an important background not modeled in GENIE 2.8.4. In particular, single K^+ production off a bound neutron, $\nu_\mu n \to \mu^- K^+ n$, has the same apparent signature as the coherent reaction if the neutron does not interact near the vertex and if the reaction happens to reconstruct to low $|t|$. To include the $\Delta S = 1$ background, we simulate the single kaon process using GENIE 2.10.0 [40] based on the model described in Ref. [23]. To preserve the total K^+ production cross section, $\Delta S = 0$ events are removed using a parameterization of the $\Delta S = 1$ to $\Delta S = 0$ cross section ratio as a function of W [1].

This measurement uses data taken by MINERvA in the NuMI beamline [41] at Fermilab. The data used in

[1] An emperical fit gives $\frac{\sigma_{\Delta S=1}(W)}{\sigma_{\Delta S=0}(W)} \approx -0.016 + \frac{0.28}{W^{1.09}}$

this analysis were taken between March 2010 and April 2012 and correspond to 3.33×10^{20} protons on target, in a ν_μ-enriched beam with a peak neutrino energy of 3.5 GeV. A Geant4-based model is used to simulate the neutrino beam. This model is constrained to reproduce thin-target hadron production measurements on carbon by the NA49 [42] and MIPP [43] experiments. The 8.5% uncertainty on the prediction of the neutrino flux is set by the precision in these measurements, and the uncertainties in the beamline focusing system [44].

The MINERvA detector is described in Ref. [45]. For this result, the interaction vertex is constrained to be within a 5.57 metric ton volume of plastic scintillator, consisting of 95% CH and 5% other materials by mass. The MINOS near detector is a magnetized iron spectrometer [46] located 2 m downstream of MINERvA and is used to reconstruct the momentum and charge of $\mu^\pm$.

We consider events with exactly two charged particle tracks originating from the neutrino interaction point: one μ^- and one K^+ candidate. The μ^- candidate must exit the back of MINERvA and match to a negatively-charged track entering the front of MINOS. Timing information is used to identify delayed decay products near the endpoint of the K^+ candidate, consistent with the 12.4 ns K^+ lifetime. The K^+ identification algorithm is described in detail in Ref. [47].

Events with evidence of nuclear break-up are rejected by considering energy deposited in a region around the interaction point. This "vertex region" extends 10 cm in each direction along the detector axis (3.5° above the beam direction), and 20 cm in the transverse direction. In signal reactions, energy in this region is due to the muon and kaon only. Additional charged hadrons deposit more energy near the vertex. Events are selected when the energy in the vertex region, E_{vtx}, is between 20 and 60 MeV, as shown in Fig. 2a. For the two-track sample, 75% of coherent events are retained by the vertex energy cut and 85% of two-track backgrounds are rejected. The prediction from simulation exceeds the data at very low vertex energy, consistent with previous MINERvA results [7, 48, 49], which require additional events with multiple nucleons beyond the GENIE prediction.

The kaon energy is measured calorimetrically by summing all energy in MINERvA not associated with the muon track. For coherent events, there are no other final state particles and this energy is due to the K^+ and the products of its interactions in the detector. A calorimetric factor of 1.2 is applied so that the kaon energy residual in the signal simulation is peaked at zero. The reconstructed neutrino energy, E_ν, is the sum of the reconstructed muon and kaon energies, $E_\mu + E_K$. The K^+ and μ^- four-vectors are used to calculate the squared four-momentum transferred to the nucleus:

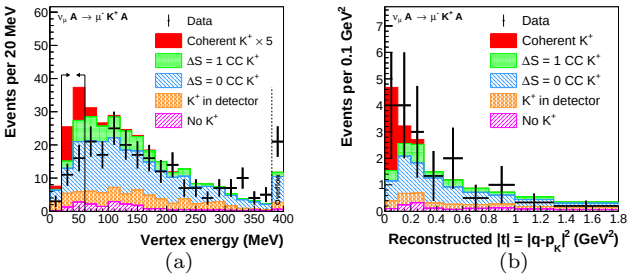

(a) (b)

FIG. 2: (a) The distribution of vertex energy before sideband tuning. The signal simulation is enhanced by a factor of 5. (b) The distribution of $|t|$ after selection on vertex energy and tuning of the background components, but before the removal of events with prompt π^0s. In both figures, data points have statistical uncertainties only.

$$|t| = -Q^2 - 2(E_K^2 - E_\nu p_K \cos\theta_K + p_\mu p_K \cos\theta_{\mu K} + m_K^2), \quad (2)$$

where Q^2 is the magnitude of the four-momentum transfer to the hadronic system, E_μ (E_K) is the muon (kaon) energy, p_μ (p_K) is the magnitude of the muon (kaon) three-momentum, θ_K is the kaon angle with respect to the neutrino beam, $\theta_{\mu K}$ is the angle between the outgoing kaon and muon, and m_K is the kaon mass.

The $|t|$ distributions for data and simulation are shown in Fig. 4. The signal simulation is normalized to the best-fit extracted from data. For simulated coherent events, 77% have reconstructed $|t| < 0.1$ GeV^2 and 94% have reconstructed $|t| < 0.2$ GeV^2. In simulated signal events where the kaon energy is underestimated, $|t|$ is overestimated. Typically this is due to a K^+ inelastic interaction in the detector. The shape in $|t|$ for background events is due to available phase space; according to the simulation 83% of background events have $|t| > 0.2$ GeV^2.

The background prediction is constrained by a sideband of events with reconstructed $|t|$ between 0.2 and 1.8 GeV^2. In the simulation, 99.5% of the events in this region are backgrounds. Prior to the background tuning, the simulation overpredicts the background rate, with 23.45 simulated events compared to 13 observed in data. The simulated background is scaled by a factor of 0.55 at all $|t|$. The kaon energy distributions in simulated background events in the sideband and signal regions are consistent.

Events that satisfy $20 < E_{vtx} < 60$ MeV typically have exactly two charged particles emerging from the neutrino interaction point, one μ^- and one K^+. Background events that pass this cut may also have neutral particles that are not observed inside the vertex region. The largest single background is $\nu_\mu n \to \mu^- K^+ \Lambda$ followed by $\Lambda \to n\pi^0$. Low vertex energy events are visually scanned

	Low E_{vtx} $\|t\| < 1.8$	$\|t\| < 0.2$	No π^0 (scan)
Best-fit signal	4.05	3.80	3.77
$\Delta S = 0$	8.88 ± 2.58	2.16 ± 0.65	0.58 ± 0.20
$\Delta S = 1$ incoherent	3.34 ± 0.97	0.87 ± 0.26	0.69 ± 0.21
K^+ in detector	2.90 ± 0.84	0.78 ± 0.23	0.36 ± 0.12
No K^+	1.89 ± 0.55	0.30 ± 0.09	0.14 ± 0.05
Total sim. bkg.	17.01 ± 4.94	4.11 ± 1.20	1.77 ± 0.53
Data	21	8	6

TABLE I: Counts for events with one μ^- and one K^+ candidate after each step in the coherent selection. The $20 < E_{vtx} < 60$ MeV cut is applied for all categories. These numbers include the scale factor of 0.55 ± 0.15 derived from the high-$|t|$ sideband. The signal is scaled to the best-fit of the unbinned likelihood fit described in the text. Backgrounds due to "K^+ in detector" arise when π^+ or K^0 interact and produce K^+.

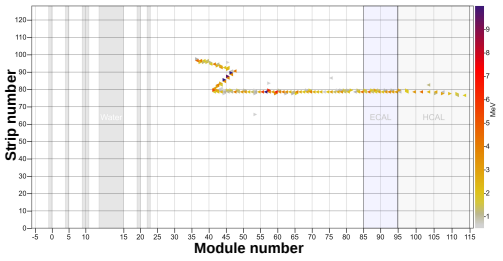

(a)

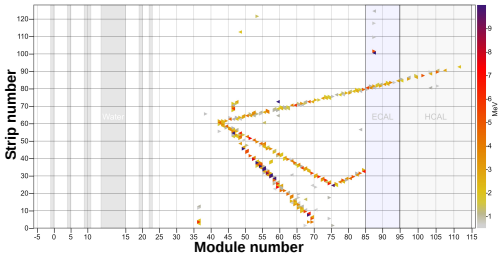

(b)

FIG. 3: (a) An event candidate in the data that is not rejected in the scan as having a π^0 candidate, compared to (b) an event that is rejected. The rejected event clearly has a photon candidate, the widest angle track in the displayed view that is detatched from the neutrino interaction point and points back to the $\mu^- K^+$ vertex and not to a point of an inelastic interaction along the K^+ track. In this event display of hits in the vertically oriented scintillator strips of the detector, the neutrino beam enters from the left, and the tracks that exit out the right of the detector are μ^-.

to remove events with an electromagnetic shower which clearly points back to the neutrino interaction point. The shower is due to the pair conversion of a photon from the decay $\pi^0 \to \gamma\gamma$. Examples of low vertex energy events with and without showers are shown in Fig. 3. Events are rejected only if the direction of the shower can be determined in order to avoid removing events where the K^+ interacts inside the detector and produces a π^0 or photon.

Scanning samples contained a mixture of simulated signal and background, and data events such that the scanner had no knowledge of whether any given event was from data or simulation. After scanning, 99% of signal events are accepted. The small inefficiency is due to π^0 produced by K^+ interactions very near the neutrino interaction point. Only 27% of $\Delta S = 0$ background events are accepted, along with 80% of $\Delta S = 1$ and 46% of other backgrounds. At low vertex energy, $\Delta S = 1$ events are dominated by $\nu_\mu n \to \mu^- K^+ n$. These events are rejected when the products of a neutron interaction in the detector point back to the neutrino interaction point. More often, the neutron interaction produces a low-energy proton for which a direction cannot be determined, and the event is accepted. The scan acceptance is consistent with no $|t|$ dependence. Two independent scanners agreed on signal efficiency, but differed on $\Delta S = 0$ background efficiencies. However, the differences applied to both data and simulation, and in the end, the two scan results give the same sensitivity to a coherent K^+ signal.

A summary of selection cuts is given in Table I. The 28% statistical uncertainty on the data in the sideband region and the 8.5% uncertainty on the integrated flux prediction [50] are fully correlated between the event categories. An uncertainty on the shape of the $|t|$ distribution is evaluated separately for each category by varying parameters in GENIE by their uncertainties [14] and computing the ratio of the prediction in the sideband and signal regions. The statistical uncertainty on the scan acceptance probability is 15% for $\Delta S = 0$ backgrounds, 6% for $\Delta S = 1$ incoherent, and 17% for the other categories.

Diffractive production of K^+ from the free protons, $\nu_\mu p \to \mu^- K^+ p$, would also produce K^+ at low $|t|$. These events have a recoiling proton with kinetic energy $T_p > m_K^4/(8E_K^2 m_p)$, which will most likely leave sufficient energy to fail the vertex energy cut. Thus the events are more likely coherent scattering from carbon.

We perform an unbinned maximum likelihood fit [51] to the signal candidates with $|t| < 0.2$ GeV^2. The background normalization is fixed within uncertainties by the high-$|t|$ sideband constraint. The only free parameter in the fit is the expected number of signal events for $|t| < 0.2$ GeV^2. Figure 4 shows the distribution of $|t|$ for these candidate events. The integrated number of signal events with $|t| < 0.2$ GeV^2 from this fit is $3.77^{+2.64}_{-1.93}$ events, where the uncertainty is the change to the number of signal events required to increase the quantity of twice the log-likelihood by one unit. The log-likelihood ratio is shown as a function of the number of coherent events in Fig. 4. We compare the ratio of likelihoods of the null hypothesis of zero signal events to the best fit of 3.77, and find a p-value of 0.28% including systematic uncertainties, equivalent to a 3.0 standard deviation exclusion of the null hypothesis of no coherent kaon production. The integrated number of predicted background

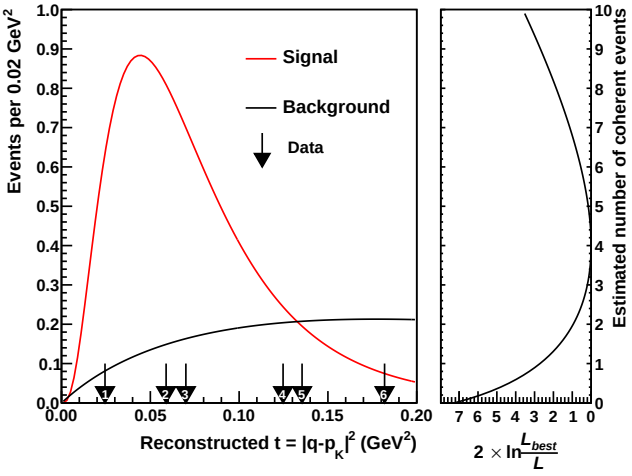

FIG. 4: (Left) $|t|$ for selected events after all selections, $|t| < 0.2$ GeV^2 compared to expected distributions for the signal and background. The normalization of the background is fixed by tuning to the high-$|t|$ sideband, while the normalization of the signal is the output of the fit. The data follow the sum of the signal and background. (Right) Twice the log of the ratio of the likelihood at best fit, L_{best}, to the likelihood, L, as a function of the estimated number of coherent events. This quantity is determined by summing over the six data events and does not include systematic uncertainties.

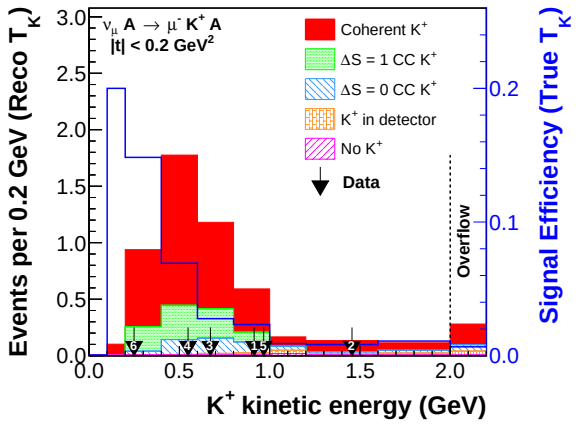

FIG. 5: The reconstructed kaon kinetic energy distribution for all accepted events in the $|t| < 0.2$ GeV^2 signal region. Event numbers correspond to the same events in Fig. 4. The vertical scale on the right side corresponds to the blue curve, which represents the reconstruction efficiency as a function of true kaon kinetic energy.

events with $|t| < 0.2$ GeV^2 is 1.77 ± 0.53. Even without considering the shape, the observation of six events in data disfavors the null hypothesis.

The number of observed events predicted on the $(1.52 \pm 0.03) \times 10^{29}$ carbon nuclei in the fiducial volume of the detector can be compared with a model prediction of the cross section using information about the neutrino flux and the acceptance for coherent K^+ events, where the latter is almost completely determined by the energy of the final state kaon. The K^+ kinetic energy distribution of selected events with reconstructed $|t| < 0.2$ GeV^2 is shown in Fig. 5. The distribution of the six data events is harder than what would be expected for background events. This information is not used in the extraction of the p-value of 0.28% for the background-only hypothesis. A total cross section cannot be derived from these data because the total acceptance depends strongly on the true kaon energy distribution, which may not be correct in our signal model.

In conclusion, evidence for coherent neutrino production of K^+ on carbon nuclei has been observed for the first time at 3.0σ significance by selecting events with a $\mu^- K^+$ final state, low momentum transfer to the nucleus, and no evidence of nuclear breakup. This evidence is consistent with the Cabibbo-suppressed analog of coherent pion production, arising from an off-shell W boson converting in the vacuum to a pseudoscalar meson, and very inconsistent with any other mechanism that does not have a Cabibbo-suppressed analog.

This work was supported by the Fermi National Accelerator Laboratory under US Department of Energy contract No. DE-AC02-07CH11359 which included the MINERvA construction project. Construction support was also granted by the United States National Science Foundation under Award PHY-0619727 and by the University of Rochester. Support for participating scientists was provided by NSF and DOE (USA), by CAPES and CNPq (Brazil), by CoNaCyT (Mexico), by CONICYT (Chile), by CONCYTEC, DGI-PUCP and IDI/IGI-UNI (Peru), and by Latin American Center for Physics (CLAF). One of us (Z.W.) gratefully acknowledges support from a University of Rochester REACH fellowship. We thank the MINOS Collaboration for use of its near detector data. We acknowledge the dedicated work of the Fermilab staff responsible for the operation and maintenance of the NuMI beamline, MINERvA and MINOS detectors and the physical and software environments that support scientific computing at Fermilab.

* now at SLAC National Accelerator Laboratory, Stanford, CA 94309, USA
† now at University of Houston, Houston, TX 77204, USA
‡ now at Illinois Institute of Technology, Chicago, IL 60616, USA
§ now at Iowa State University, Ames, IA 50011, USA
¶ now at University of Michigan, Ann Arbor, MI 48109, USA
** also at Department of Physics, University of Antananarivo, Madagascar
†† now at Fermi National Accelerator Laboratory, Batavia, IL 60510, USA
‡‡ now at Tufts University, Medford, MA 02155, USA
§§ Deceased

[1] H. Grabosch *et al.* (SKAT Collaboration), Z.Phys. **C31**, 203 (1986).

[2] P. Marage *et al.* (BEBC WA59 Collaboration), Z.Phys. **C31**, 191 (1986).
[3] P. Allport *et al.* (BEBC WA59 Collaboration), Z.Phys. **C43**, 523 (1989).
[4] P. Vilain *et al.* (CHARM-II Collaboration), Phys.Lett. **B313**, 267 (1993).
[5] M. Hasegawa *et al.* (K2K Collaboration), Phys. Rev. Lett. **95**, 252301 (2005), arXiv:hep-ex/0506008 [hep-ex] .
[6] K. Hiraide *et al.* (SciBooNE Collaboration), Phys. Rev. **D78**, 112004 (2008), arXiv:0811.0369 [hep-ex] .
[7] A. Higuera, A. Mislivec, *et al.* (MINERvA Collaboration), Phys. Rev. Lett. **113**, 261802 (2014).
[8] R. Acciarri *et al.* (ArgoNeuT Collaboration), (2014), arXiv:1408.0598 [hep-ex] .
[9] S. L. Adler, Phys. Rev. **135**, B963 (1964).
[10] C. Piketty and L. Stodolsky, Nucl. Phys. **B15**, 571 (1970).
[11] K. Lackner, Nucl. Phys. **B153**, 526 (1979).
[12] D. Rein and L. M. Sehgal, Nucl. Phys. **B223**, 29 (1983).
[13] C. Berger and L. Sehgal, Phys. Rev. **D79**, 053003 (2009), arXiv:0812.2653 [hep-ph] .
[14] C. Andreopoulos, A. Bell, D. Bhattacharya, F. Cavanna, J. Dobson, S. Dytman, H. Gallagher, P. Guzowski, R. Hatcher, P. Kehayias, A. Meregaglia, D. Naples, G. Pearce, A. Rubbia, M. Whalley, and T. Yang, Nuclear Instruments and Methods in Physics Research Section A: Accelerators, Spectrometers, Detectors and Associated Equipment **614**, 87 (2010), Program version 2.8.4 used here.
[15] Y. Hayato, Acta Phys.Polon. **B40**, 2477 (2009).
[16] D. Casper, Nucl.Phys.Proc.Suppl. **112**, 161 (2002), arXiv:hep-ph/0208030 [hep-ph] .
[17] T. Golan, C. Juszczak, and J. T. Sobczyk, Phys. Rev. **C86**, 015505 (2012), arXiv:1202.4197 [nucl-th] .
[18] S. Gershtein, Y. Y. Komachenko, and M. Y. a. Khlopov, Sov. J. Nucl. Phys. **32**, 861 (1980).
[19] A. Belkov and B. Kopeliovich, Sov. J. Nucl. Phys. **46**, 499 (1987).
[20] E. Paschos and D. Schalla, Phys. Rev. **D80**, 033005 (2009), arXiv:0903.0451 [hep-ph] .
[21] D. Rein and L. Sehgal, Phys. Lett. **B657**, 207 (2007), arXiv:hep-ph/0606185 [hep-ph] .
[22] A. Higuera and E. Paschos, Eur. Phys. J. Plus **129**, 43 (2014), arXiv:1311.5149 [hep-ph] .
[23] M. Rafi Alam, I. Ruiz Simo, M. Sajjad Athar, and M. J. Vicente Vacas, Phys. Rev. D **82**, 033001 (2010).
[24] L. Alvarez-Ruso, J. Nieves, I. R. Simo, M. Valverde, and M. J. Vicente Vacas, Phys. Rev. **C87**, 015503 (2013), arXiv:1205.4863 [nucl-th] .
[25] B. Gobbi, W. Hakel, J. L. Rosen, and S. Shapiro, Phys. Rev. Lett. **29**, 1278 (1972).
[26] M. M. Sternheim and R. R. Silbar, Ann. Rev. Nucl. Part. Sci. **24**, 249 (1974).
[27] K. A. Olive *et al.* (Particle Data Group), Chin. Phys. **C38**, 090001 (2014).
[28] B. Kopeliovich, I. Potashnikova, and I. Strakovsky, private communication.
[29] D. Rein and L. M. Sehgal, Annals Phys. **133**, 79 (1981).
[30] A. Bodek, I. Park, and U.-K. Yang, Nucl. Phys. Proc. Suppl. **139**, 113 (2005), arXiv:hep-ph/0411202 [hep-ph] .
[31] T. Yang, C. Andreopoulos, H. Gallagher, K. Hoffmann, and P. Kehayias, Eur.Phys.J. **C63**, 1 (2009), arXiv:0904.4043 [hep-ph] .
[32] Z. Koba, H. B. Nielsen, and P. Olesen, Nucl. Phys. **B40**, 317 (1972).
[33] T. Sjostrand, S. Mrenna, and P. Skands, JHEP **0605**, 026 (2006), arXiv:hepph/0603175 [hepph] .
[34] G. T. Jones *et al.*, Z. Phys. **C57**, 197 (1993).
[35] D. Allasia *et al.* (Amsterdam-Bergen-Bologna-Padua-Pisa-Saclay-Turin), Nucl. Phys. **B224**, 1 (1983).
[36] P. Bosetti *et al.* (Aachen-Bonn-CERN-Democritos-London-Oxford-Saclay), Nucl. Phys. **B209**, 29 (1982).
[37] S. Willocq *et al.* (WA59), Z. Phys. **C53**, 207 (1992).
[38] N. J. Baker *et al.*, Phys. Rev. **D34**, 1251 (1986).
[39] D. DeProspo *et al.* (E632), Phys. Rev. **D50**, 6691 (1994).
[40] R. Alam *et al.*, (2015), arXiv:1512.06882 [hep-ph] .
[41] P. Adamson *et al.*, Nucl. Instrum. Meth. A **806**, 279 (2016), arXiv:1507.06690 [physics.acc-ph] .
[42] C. Alt *et al.* (NA49 Collaboration), Eur. Phys. J. **C49**, 897 (2007), arXiv:hep-ex/0606028 [hep-ex] .
[43] A. V. Lebedev, *Ratio of pion kaon production in proton carbon interactions*, Ph.D. thesis, Harvard University (2007).
[44] Z. Pavlovic, *Observation of Disappearance of Muon Neutrinos in the NuMI Beam*, Ph.D. thesis, University of Texas (2008).
[45] L. Aliaga *et al.* (MINERvA Collaboration), Nucl.Instrum.Meth. **A743**, 130 (2014), arXiv:1305.5199 [physics.ins-det] .
[46] D. G. Michael *et al.* (MINOS Collaboration), Nucl.Instrum.Meth. **A596**, 190 (2008), arXiv:0805.3170 [physics.ins-det] .
[47] C. Marshall *et al.* (MINERvA Collaboration), (2016), arXiv:1604.03920 [hep-ex] .
[48] G. Fiorentini, D. Schmitz, *et al.* (MINERvA Collaboration), Phys. Rev. Lett. **111**, 022502 (2013), arXiv:1305.2243 [hep-ex] .
[49] P. A. Rodrigues *et al.* (MINERvA Collaboration), Phys. Rev. Lett. **116**, 071802 (2016).
[50] L. Aliaga Soplin, Ph.D. thesis, William and Mary (2016).
[51] K. Olive *et al.* (Particle Data Group), Chinese Physics C **38**, 090001 (2014).